

# Photon polarization effects in polarized electron-positron pair production in a strong laser field

Ya-Nan Dai,<sup>1</sup> Bai-Fei Shen,<sup>1</sup> Jian-Xing Li,<sup>2</sup> Rashid Shaisultanov,<sup>3,4</sup> Karen Z. Hatsagortsyan,<sup>3</sup> Christoph H. Keitel,<sup>3</sup> and Yue-Yue Chen<sup>1, a)</sup>

<sup>1)</sup>*Department of Physics, Shanghai Normal University, Shanghai 200234, China*

<sup>2)</sup>*School of Physics, Xi'an Jiaotong University, Xi'an 710049, China*

<sup>3)</sup>*Max-Planck-Institut für Kernphysik, Saupfercheckweg 1, 69117 Heidelberg, Germany*

<sup>4)</sup>*Helmholtz-Zentrum Dresden-Rossendorf, Bautzner Landstraße 400, 01328 Dresden, Germany*

(Dated: 11 October 2021)

Deep understanding of photon polarization impact on pair production is essential for the efficient creation of laser driven polarized positron beams, and demands a complete description of polarization effects in strong-field QED processes. We investigate, employing fully polarization resolved Monte Carlo simulations, the correlated photon and electron (positron) polarization effects in multiphoton Breit-Wheeler pair production process during the interaction of an ultra-relativistic electron beam with a counterpropagating elliptically polarized laser pulse. We showed that the polarization of  $e^-e^+$  pairs is degraded by 35%, when the polarization of the intermediate photon is resolved, accompanied with an approximately 13% decrease of the pair yield. Moreover, the polarization direction of energetic positrons in small angle region is reversed, which originates from the pair production of hard photons with polarization parallel with electric field.

## I. INTRODUCTION

Polarized positron beams are a powerful tool for exploration of fine structure of matter, in particular, for probing nuclear constituents<sup>1</sup>, and testing the validity of the Standard Model<sup>2</sup> of particle physics via weak and electromagnetic interactions. The natural decay of some radio-isotopes generates polarized positrons with polarization up to 40%<sup>3</sup>, but the flux is too low for further acceleration and applications. Positrons can also be polarized in a storage ring due to spin-flips at photon emissions (Sokolov-Ternov effect)<sup>4-8</sup>, which however, is a slow process lasting at least several minutes and can be realized in a large scale storage ring facilities. At particle accelerators polarized  $e^-e^+$  pairs are commonly produced by scattering of circularly polarized gamma-photons in a high-Z material via Bethe-Heitler process<sup>9-11</sup>, while the luminosity of positrons is limited because of constraints on the target thickness<sup>12</sup>, and the required intense flux of sufficiently energetic photons with a high degree of circular polarization is challenging to produce<sup>13</sup>.

Recently, the rapid development of petawatt (PW) laser technology<sup>14-19</sup> and laser wakefield acceleration<sup>20,21</sup> stimulate distinct interest towards development of polarized positron source via nonlinear Breit-Wheeler (NBW) process<sup>22-29</sup>. The positrons created in a strong laser field can be polarized due to the energetically preferred orientation of the positron spin along the local magnetic field. However, the challenge is that in a symmetric laser field (e.g. in a monochromatic laser field) the polarization of positrons created in different laser half-cycles oscillates following the laser magnetic field and averages out to zero for the total beam. Thus, to achieve net polarization of the created positrons, it is necessary to use an asymmetric laser field. For instance,

recently a two-color laser field has been proposed to exploit for ultrafast generation of highly polarized electron<sup>30,31</sup> and positron beams<sup>24</sup>. Another efficient way for laser driven generation of polarized electrons (positrons) has been also demonstrated<sup>23,32</sup>, employing the spin-dependent radiation reaction in an elliptically polarized laser pulse to split the electron (positron) beam into two oppositely transversely polarized parts. Laser driven positron generation schemes provide a promising avenue for high current, highly-polarized positron sources.

Usually the gamma-photon which creates a pair in NBW process is generated due to the Compton scattering of incoming electron beam off a counterpropagating laser field. In most of studies, the gamma-photon have been assumed unpolarized and the NBW probability has been averaged over the photon polarization<sup>23,24,30,31</sup>. In reality the intermediate gamma-photon is partially polarized, which has consequences for further pair production process<sup>25,33,34</sup>. In particular, the decrease of the pair density with the inclusion of photon polarization has been shown in analytical QED calculations<sup>33</sup> averaged by the lepton spins, which is confirmed by more accurate spin resolved Monte Carlo simulations<sup>34</sup>. Moreover, highly polarized gamma-photons can be obtained with polarized seed electrons<sup>13</sup>, which in further NBW process may create highly polarized positrons, as it is shown in the Monte Carlo simulation<sup>25</sup> with the use of a simplified pair production probability summed up over final spin states of either electron or positron. Therefore, including photon polarization in the description of NBW process is mandatory for a reliable prediction of parameters of the laser driven polarized positron source. The study of fully polarization resolved NBW is also of pure theoretical interest, providing insight on correlations of electrons, positrons and photons polarization in strong-field pair production processes.

Analytical description of strong-field QED processes is possibly only in a case of a plane wave laser field<sup>22,35-39</sup>. For QED processes in more realistic scenarios including

<sup>a)</sup>Electronic mail: yueyuechen@shnu.edu.cn

focused laser fields and laser-plasma interaction, a Monte Carlo method has been developed<sup>40-42</sup>, which is based on the local constant field approximation (LCFA)<sup>43-49</sup>, applicable for intense laser-plasma<sup>40-42,50</sup>/ultra-relativistic electrons interactions<sup>13,24,25,34</sup>. Recently, the QED Monte Carlo method has been generalized to include spin of involved leptons<sup>24,32</sup> and polarization of emitted or absorbed photons<sup>13,25,34,51</sup>. A numerical approach suitable for treating polarization effects beyond LCFA and plane wave approximations at intermediate laser intensities has been developed<sup>52,53</sup> for strong-field pair production process within the semiclassical formalism of Baier-Katkov.

In this paper, we investigate the interaction of an ultrarelativistic electron beam head-on colliding with an ultraintense laser pulse and focus on the effects of photon polarization in NBW pair production process. To provide an accurate analysis of the produced pair polarization, we employ fully polarization resolved NBW probabilities, i.e., resolved as in incoming photon polarization as well as in the created electron and positron polarizations. The probabilities are derived with Baier-Katkov QED operator method<sup>43,54</sup> within LCFA. and have been included into the recently developed laser-electron beam simulation code<sup>25</sup>. We consider a scheme where the initial electrons are transversely polarized and the laser field is elliptically polarized. With the fully polarization-resolved Monte Carlo method, we find that the polarization of the produced positrons is highly dependent on the polarization of parent photons. In particular, the polarization of positrons is reduced by 35% since the emitted photons is partially polarized along electric field direction, and that the angular distribution of positron polarization exhibits an abnormal twist near small angle region, which originates from pair production of highly polarized photons at the high energy end of the spectrum.

## II. SIMULATION METHOD

In this section, we analysis the correlation of photon and positron/electron polarization based on fully polarization resolved probabilities and briefly elaborate on the Monte Carlo method used for simulation.

### A. Photon polarization resolved radiation probability

Here, we provide probabilities of a polarized photon emission with a polarized electron. Let us assume that the polarization of the emitted photon is  $\vec{e} = a_1 \vec{e}_1 + a_2 \vec{e}_2$ , where

$$\vec{e}_1 = \vec{s} - (\vec{n}\vec{s})\vec{s}, \quad \vec{e}_2 = \vec{n} \times \vec{e}_1. \quad (1)$$

$\vec{n} = \vec{k}/|\vec{k}|$  and  $\vec{s} = \vec{w}/|\vec{w}|$  are the unit vectors along the photon emission and acceleration directions, respectively. The photon

polarization resolved emission probability reads

$$\begin{aligned} dW_r &= \frac{1}{2} (dW_{11} + dW_{22}) + \frac{\xi_1}{2} (dW_{11} - dW_{22}) \\ &\quad - i \frac{\xi_2}{2} (dW_{21} - dW_{12}) + \frac{\xi_3}{2} (dW_{11} - dW_{22}) \\ &= \frac{1}{2} (F_0 + \xi_1 F_1 + \xi_2 F_2 + \xi_3 F_3), \end{aligned} \quad (2)$$

where  $\xi_i$  ( $i = 1, 2, 3$ ) are Stokes parameters with respect to axes  $(\vec{e}_1, \vec{e}_2, \vec{n})$ , and

$$\begin{aligned} F_0 &= \frac{\alpha}{2\sqrt{3}\pi\gamma^2} d\omega \left\{ \left( \frac{\varepsilon^2 + \varepsilon'^2}{\varepsilon\varepsilon'} K_{\frac{2}{3}}(z_q) - \int_{z_q}^{\infty} dx K_{\frac{1}{3}}(x) \right) \right. \\ &\quad + \left( 2K_{\frac{2}{3}}(z_q) - \int_{z_q}^{\infty} dx K_{\frac{1}{3}}(x) \right) (\vec{\zeta}_i \vec{\zeta}_f) \\ &\quad - K_{\frac{1}{3}}(z_q) \left( \frac{\omega}{\varepsilon} (\vec{\zeta}_i \vec{b}) + \frac{\omega}{\varepsilon'} (\vec{\zeta}_f \vec{b}) \right) \\ &\quad \left. + \frac{\omega^2}{\varepsilon'\varepsilon} \left( K_{\frac{2}{3}}(z_q) - \int_{z_q}^{\infty} dx K_{\frac{1}{3}}(x) \right) (\vec{\zeta}_i \vec{v}) (\vec{\zeta}_f \vec{v}) \right\}, \end{aligned} \quad (3)$$

$$\begin{aligned} F_3 &= \frac{\alpha}{2\sqrt{3}\pi\gamma^2} d\omega \left\{ K_{\frac{2}{3}}(z_q) + \frac{\varepsilon^2 + \varepsilon'^2}{2\varepsilon'\varepsilon} K_{\frac{2}{3}}(z_q) (\vec{\zeta}_i \vec{\zeta}_f) \right. \\ &\quad - \left[ \frac{\omega}{\varepsilon'} (\vec{\zeta}_i \vec{b}) + \frac{\omega}{\varepsilon} (\vec{\zeta}_f \vec{b}) \right] K_{\frac{1}{3}}(z_q) \\ &\quad + \frac{\omega^2}{2\varepsilon'\varepsilon} \left( -K_{\frac{2}{3}}(z_q) (\vec{\zeta}_i \vec{v}) (\vec{\zeta}_f \vec{v}) \right. \\ &\quad \left. + \int_{z_q}^{\infty} dx K_{\frac{1}{3}}(x) \left( [\vec{\zeta}_i \vec{b}] [\vec{\zeta}_f \vec{b}] - (\vec{\zeta}_i \vec{s}) (\vec{\zeta}_f \vec{s}) \right) \right) \left. \right\}, \end{aligned} \quad (4)$$

$$\begin{aligned} F_1 &= \frac{\alpha}{2\sqrt{3}\pi\gamma^2} d\omega \left\{ \frac{\varepsilon^2 - \varepsilon'^2}{2\varepsilon'\varepsilon} K_{\frac{2}{3}}(z_q) (\vec{v} [\vec{\zeta}_f \times \vec{\zeta}_i]) \right. \\ &\quad + \left[ \frac{\omega}{\varepsilon'} (\vec{\zeta}_i \vec{s}) + \frac{\omega}{\varepsilon} (\vec{\zeta}_f \vec{s}) \right] K_{\frac{1}{3}}(z_q) \\ &\quad \left. - \frac{\omega^2}{2\varepsilon'\varepsilon} \int_{z_q}^{\infty} dx K_{\frac{1}{3}}(x) \left( (\vec{\zeta}_i \vec{s}) (\vec{\zeta}_f \vec{b}) + (\vec{\zeta}_i \vec{b}) (\vec{\zeta}_f \vec{s}) \right) \right\}, \end{aligned} \quad (5)$$

$$\begin{aligned} F_2 &= -\frac{\alpha}{2\sqrt{3}\pi\gamma^2} d\omega \left\{ \frac{\varepsilon^2 - \varepsilon'^2}{2\varepsilon'\varepsilon} K_{\frac{1}{3}}(z_q) (\vec{s} [\vec{\zeta}_f \times \vec{\zeta}_i]) \right. \\ &\quad + \left[ -\frac{\varepsilon^2 - \varepsilon'^2}{\varepsilon'\varepsilon} K_{\frac{2}{3}}(z_q) + \frac{\omega}{\varepsilon} \int_{z_q}^{\infty} dx K_{\frac{1}{3}}(x) \right] (\vec{\zeta}_i \vec{v}) \\ &\quad + \left[ -\frac{\varepsilon^2 - \varepsilon'^2}{\varepsilon'\varepsilon} K_{\frac{2}{3}}(z_q) + \frac{\omega}{\varepsilon'} \int_{z_q}^{\infty} dx K_{\frac{1}{3}}(x) \right] (\vec{\zeta}_f \vec{v}) \\ &\quad \left. + \frac{\omega^2}{2\varepsilon'\varepsilon} K_{\frac{1}{3}}(z_q) \left( (\vec{\zeta}_i \vec{v}) (\vec{\zeta}_f \vec{b}) + (\vec{\zeta}_i \vec{b}) (\vec{\zeta}_f \vec{v}) \right) \right\}, \end{aligned} \quad (6)$$

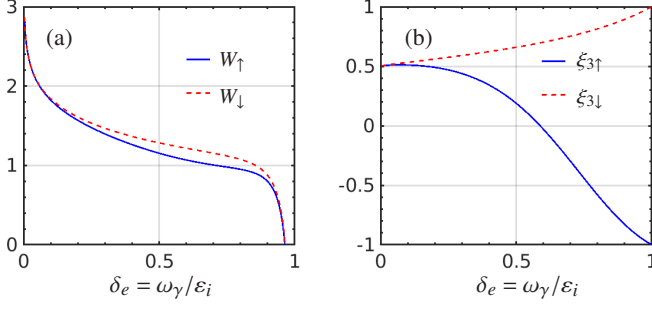


FIG. 1. (a) The photon emission probability  $\log_{10} W_i$  (arb. units), and (b) Stokes parameter  $\xi_{3i}$  ( $i \in \uparrow, \downarrow$ ) vs emitted photon energy  $\delta_e = \omega_\gamma/\epsilon_i$  for  $\chi_e = 10$ .  $i$  denotes the electron spin before the emission with respect to the magnetic field direction.

where  $\vec{v} = \frac{\vec{v}}{v}$ ,  $\vec{b} = \vec{v} \times \vec{s}$ ,  $z_q = \frac{2}{3} \frac{\omega}{\chi_e \epsilon'}$ ,  $\epsilon$  and  $\epsilon'$  are the energy of the emitting particle before and after emission, respectively,  $\vec{\zeta}_i$  and  $\vec{\zeta}_f$  are the spin vectors before and after emission, respectively,  $\omega$  is the emitted photon energy.

The emission probability and the polarization of the emitted photon both depend on the initial electron spin  $\vec{\zeta}_i$ . For instance, the emission probability is larger for the spin-down electron, with respect to magnetic field direction in the rest frame of the electron, than for the spin-up electrons, as shown in Fig. 1(a). The dependence of polarization of the photon on  $\vec{\zeta}_i$  is more remarkable, as shown in Fig. 1 (b). For low energy region, the Stokes parameter  $\xi_3 \sim 0.5$  regardless of the initial electron spin. However, with the increase of the emitted photons energy,  $\xi_3$  increases up to  $\xi_3 = 1$  for the spin-up electron, while decreases to  $\xi_3 = -1$  for the opposite case.

## B. Photon polarization resolved pair production probabilities

Here, we provide probability of a polarized electron-positron pair production with a polarized photon.

The polarization of the photon is defined as follows:

$$\vec{e} = a_1 \vec{e}_1 + a_2 \vec{e}_2 \quad (7)$$

$$\vec{e}_1 = \frac{\vec{E} - \vec{n}(\vec{n} \cdot \vec{E}) + \vec{n} \times \vec{B}}{|\vec{E} - \vec{n}(\vec{n} \cdot \vec{E}) + \vec{n} \times \vec{B}|}, \quad (8)$$

$$\vec{e}_2 = \vec{n} \times \vec{e}_1, \vec{n} = \frac{\vec{k}}{|\vec{k}|}. \quad (9)$$

The pair production rate of the polarized photon takes the form

$$\begin{aligned} dW_p &= \frac{1}{2} (dW^{(11)} + dW^{(22)}) + \frac{\xi_1}{2} (dW^{(11)} - dW^{(22)}) \\ &\quad - i \frac{\xi_2}{2} (dW^{(21)} - dW^{(12)}) + \frac{\xi_3}{2} (dW^{(11)} - dW^{(22)}) \\ &= \frac{1}{2} (G_0 + \xi_1 G_1 + \xi_2 G_2 + \xi_3 G_3), \end{aligned} \quad (10)$$

where  $\xi_i = \frac{G_i}{G_0}$ ,  $i = 1, 2, 3$  are the Stokes parameters.

$$\begin{aligned} G_0 &= \frac{\alpha m^2 d\epsilon}{2\sqrt{3}\pi\omega^2} \left\{ \int_{z_p}^{\infty} dx K_{\frac{1}{3}}(x) + \frac{\epsilon_+^2 + \epsilon^2}{\epsilon_+ \epsilon} K_{\frac{2}{3}}(z_p) \right\} \\ &\quad + \left\{ \int_{z_p}^{\infty} dx K_{\frac{1}{3}}(x) - 2K_{\frac{2}{3}}(z_p) \right\} (\vec{\zeta}_- \cdot \vec{\zeta}_+) \\ &\quad + \left[ \frac{\omega}{\epsilon_+} (\vec{\zeta}_+ \cdot \vec{b}) - \frac{\omega}{\epsilon} (\vec{\zeta}_- \cdot \vec{b}) \right] K_{\frac{1}{3}}(z_p) \\ &\quad + \left\{ \frac{\epsilon_+^2 + \epsilon^2}{\epsilon \epsilon_+} \int_{z_p}^{\infty} dx K_{\frac{1}{3}}(x) - \frac{(\epsilon_+ - \epsilon)^2}{\epsilon \epsilon_+} K_{\frac{2}{3}}(z_p) \right\} (\vec{\zeta}_- \cdot \vec{v}) (\vec{\zeta}_+ \cdot \vec{v}) \end{aligned} \quad (11)$$

$$\begin{aligned} G_3 &= \frac{\alpha m^2 d\epsilon}{2\sqrt{3}\pi\omega^2} \left\{ -K_{\frac{2}{3}}(z_p) + \frac{\epsilon_+^2 + \epsilon^2}{2\epsilon_+ \epsilon} K_{\frac{2}{3}}(z_p) (\vec{\zeta}_- \cdot \vec{\zeta}_+) \right. \\ &\quad + \left[ -\frac{\omega}{\epsilon} (\vec{\zeta}_+ \cdot \vec{b}) + \frac{\omega}{\epsilon_+} (\vec{\zeta}_- \cdot \vec{b}) \right] K_{\frac{1}{3}}(z_p) \\ &\quad - \frac{(\epsilon_+ - \epsilon)^2}{2\epsilon_+ \epsilon} K_{\frac{2}{3}}(z_p) (\vec{\zeta}_- \cdot \vec{v}) (\vec{\zeta}_+ \cdot \vec{v}) \\ &\quad \left. + \frac{\omega^2}{2\epsilon_+ \epsilon} \int_{z_p}^{\infty} dx K_{\frac{1}{3}}(x) [(\vec{\zeta}_- \cdot \vec{b})(\vec{\zeta}_+ \cdot \vec{b}) - (\vec{\zeta}_- \cdot \vec{s})(\vec{\zeta}_+ \cdot \vec{s})] \right\} \quad (12) \end{aligned}$$

$$\begin{aligned} G_1 &= \frac{\alpha m^2 d\epsilon}{2\sqrt{3}\pi\omega^2} \left\{ -\frac{\epsilon_+^2 - \epsilon^2}{2\epsilon_+ \epsilon} K_{\frac{2}{3}}(z_p) \vec{v} (\vec{\zeta}_+ \times \vec{\zeta}_-) \right. \\ &\quad + \left[ \frac{\omega}{\epsilon} (\vec{\zeta}_+ \cdot \vec{s}) - \frac{\omega}{\epsilon_+} (\vec{\zeta}_- \cdot \vec{s}) \right] K_{\frac{1}{3}}(z_p) \\ &\quad \left. - \frac{\omega^2}{2\epsilon_+ \epsilon} \int_{z_p}^{\infty} dx K_{\frac{1}{3}}(x) [(\vec{\zeta}_- \cdot \vec{b})(\vec{\zeta}_+ \cdot \vec{s}) + (\vec{\zeta}_- \cdot \vec{s})(\vec{\zeta}_+ \cdot \vec{b})] \right\} \quad (13) \end{aligned}$$

$$\begin{aligned} G_2 &= \frac{\alpha m^2 d\epsilon}{2\sqrt{3}\pi\omega^2} \left\{ -\frac{\omega^2}{2\epsilon_+ \epsilon} K_{\frac{1}{3}}(z_p) [\vec{s} (\vec{\zeta}_- \times \vec{\zeta}_+)] \right. \\ &\quad + \left( \frac{\omega}{\epsilon_+} \int_{z_p}^{\infty} dx K_{\frac{1}{3}}(x) + \frac{\epsilon_+^2 - \epsilon^2}{\epsilon_+ \epsilon} K_{\frac{2}{3}}(z_p) \right) (\vec{\zeta}_+ \cdot \vec{v}) \\ &\quad + \left( \frac{\omega}{\epsilon} \int_{z_p}^{\infty} dx K_{\frac{1}{3}}(x) - \frac{\epsilon_+^2 - \epsilon^2}{\epsilon_+ \epsilon} K_{\frac{2}{3}}(z_p) \right) (\vec{\zeta}_- \cdot \vec{v}) \\ &\quad \left. - \frac{\epsilon_+^2 - \epsilon^2}{2\epsilon_+ \epsilon} K_{\frac{1}{3}}(z_p) [(\vec{\zeta}_- \cdot \vec{v})(\vec{\zeta}_+ \cdot \vec{b}) + (\vec{\zeta}_- \cdot \vec{b})(\vec{\zeta}_+ \cdot \vec{v})] \right\}, \quad (14) \end{aligned}$$

where  $\vec{v} = \frac{\vec{v}}{v}$  is the velocity direction of the produced pairs, which fulfills  $\vec{v}_- \approx \vec{v}_+ \approx \vec{n}$  in the relativistic case,  $\vec{s} = \frac{\vec{v}}{|\vec{v}|}$  is the acceleration direction of the produced particles,  $\vec{b} = \vec{v} \times \vec{s}$

the magnetic field direction in the rest frame of the electron/positron, the parameter  $z_p = \frac{2\omega}{3\chi_\gamma \varepsilon \varepsilon_+}$ , where  $\omega$ ,  $\varepsilon$  and  $\varepsilon_+$  are the energy of the parent photon, the produced electron and positron, respectively, the quantum strong-field parameter  $\chi_\gamma = \frac{|e|\sqrt{(F_\mu \nu k^\nu)^2}}{m^3}$ , with the four-vector  $k$  of the photon momentum. Averaging over the photon polarization yields the spin-resolved pair production probability<sup>43,55,56</sup>:  $dW_p(0) = \frac{1}{2}G_0$ .

Summing up the final spin state of electron, one can obtain the polarization of the positron depending on the photon polarization:

$$\vec{\zeta}_+^{f,\xi} = \frac{\xi_1 f_3 \frac{\omega}{\varepsilon} \vec{s} + \xi_2 \vec{v} \left( \frac{\omega}{\varepsilon_+} f_1 + \frac{\varepsilon_+^2 - \varepsilon^2}{\varepsilon \varepsilon_+} f_2 \right) + \left( \frac{\omega}{\varepsilon_+} - \xi_3 \frac{\omega}{\varepsilon} \right) \vec{b} f_3}{f_1 + \frac{\varepsilon^2 + \varepsilon_+^2}{\varepsilon \varepsilon_+} f_2 - \xi_3 f_2}. \quad (15)$$

In the case of an unpolarized photon:

$$\vec{\zeta}_+^{f,0} = \frac{\frac{\omega}{\varepsilon_+} \vec{b} f_3}{f_1 + \frac{\varepsilon^2 + \varepsilon_+^2}{\varepsilon \varepsilon_+} f_2}, \quad (16)$$

where  $f_1 = \int_{z_p}^{\infty} dx K_{\frac{1}{3}}(x)$ ,  $f_2 = K_{\frac{2}{3}}(z_p)$ ,  $f_3 = K_{\frac{1}{3}}(z_p)$ . Eqs (15) and (16) show that the photon polarization has significant effects on positron polarization  $\vec{\zeta}_+^f$ . The longitudinal polarization of positrons is completely missing if the photon polarization is averaged, while the transverse polarization either increase or decrease determined by  $\xi_1$  and  $\xi_3$ .

The correlation of the electron and positron polarizations in the pair production is analysed in Fig. 2. In the case  $\xi_1 = \xi_2 = 0$  and  $\xi_3 > 0$ , the probabilities of  $e^+e^-$  co-polarization are higher than counter-polarization with respect to magnetic field direction, i.e.  $dW_{\uparrow\uparrow}, dW_{\downarrow\downarrow} > dW_{\downarrow\uparrow}, dW_{\uparrow\downarrow}$ , as shown in Fig. 2(a). On the other hand, when  $\xi_3 < 0$ , the probability of producing an electron with spin down and positron spin up dominates, i.e.  $dW_{\downarrow\uparrow} > dW_{\downarrow\downarrow}, dW_{\uparrow\uparrow}, dW_{\uparrow\downarrow}$ , as shown in Fig. 2(b).

After integration over the electron spin, one obtain the dependence of positron spin on the positron energy and the polarization of the parent photon, as shown in Fig. 2(c). For  $\xi_3 < 0$ , positron polarization degree decreases gradually with the increase of positron energy. The domination of  $dW_{\downarrow\uparrow}$  results in a high polarization degree of positrons with spin up through the whole spectrum. While for a photon with  $\xi_3 > 0$ , the polarization of the produced positron decreases dramatically to a negative value with the increase of energy, resulting in a smaller averaged polarization compared with the case of  $\xi_3 = 0$ . Especially, when  $\xi_3 \sim 1$  shown in Fig. 2 (a), the probability  $\sum_{\zeta_-} dW_{\zeta_- \uparrow} \approx \sum_{\zeta_-} dW_{\zeta_- \downarrow}$ . The polarization of positrons in high ( $\delta_+ > 0$ ) and low energy ( $\delta_+ < 0$ ) regions cancel each other out, producing unpolarized positrons after energy integration. Therefore, if the parent photon is polarized along laser polarization direction, i.e.  $\xi_3 = 1$ , the produced pairs are unpolarized. While, if the polarization of the parent photon is orthogonal to laser polarization, i.e.  $\xi_3 = -1$ , the produced pairs have a high degree of polarization with positrons spin up and electrons spin down. After integration over the positron energy, one obtain the relation between positron polarization and polarization of its parent photon, as shown in Fig. 2 (e). The polarization of positron decreases monotonously with the

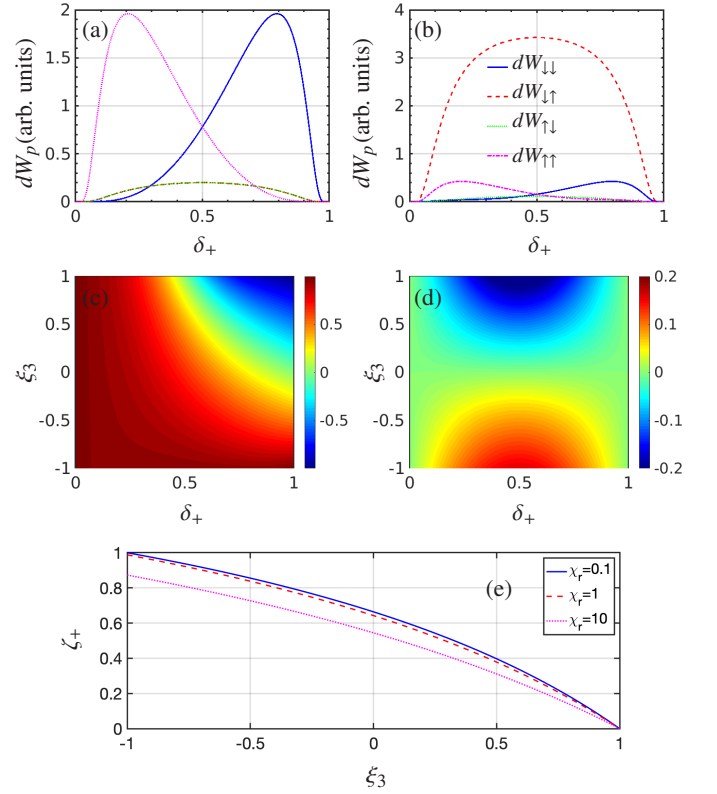


FIG. 2. The pair production probability  $dW_{\zeta_- \zeta_+}$  for the polarized photon with (a)  $\xi_1 = \xi_2 = 0, \xi_3 = 1$ , and (b)  $\xi_3 = -1$ ; (c) Positron polarization  $\zeta_+ = \sum_{\zeta_-} \frac{dW_{\zeta_- \uparrow} - dW_{\zeta_- \downarrow}}{dW_{\zeta_- \uparrow} + dW_{\zeta_- \downarrow}}$  vs  $\xi_3$  and  $\delta_+$ ; (d) Difference of the photon polarization resolved and averaged pair production probabilities  $\frac{dW_p(\xi) - dW_p(0)}{dW_p(\xi) + dW_p(0)}$  vs  $\xi_3$  and  $\delta_+$ ;  $\chi_\gamma = 3$  for (a),(b) and (c); (e)  $\zeta_+ = \sum_i \zeta_+(\delta_i) \cdot \frac{dW_p(\delta_i)}{\sum_i dW_p(\delta_i)}$  versus  $\xi_3$  for  $\chi_\gamma = 0.1$  (blue-solid),  $\chi_\gamma = 1$  (red-dashed) and  $\chi_\gamma = 10$  (magenta-dotted).

increase of  $\xi_3$ , which provides a way of estimating the polarization of the intermediate photons during nonlinear Compton scattering. For instance, if the polarization of positrons is measured to be 37% at  $\chi_\gamma = 1$ , the polarization of the intermediate photons is around  $\xi_3 = 0.5$ .

The photon polarization not only affect the polarization of produced pairs, but also the pairs density, as shown in Fig. 2 (d). When  $\xi_3 > 0$ , the pair production probability is smaller than the case where photon polarization is unresolved, i.e.  $\xi_3 = 0$ . On the contrary, the photons with  $\xi_3 < 0$  yield more pairs than the unpolarized photons.

### C. Stochastic algorithm

To simulate the nonlinear Compton scattering of a strong laser pulse at an ultrarelativistic electrons beam, we modified the three-dimensional Monte Carlo method<sup>25</sup> by employing the fully polarization resolved pair production probability given in Sec. II.B. The developed Monte-Carlo method includes the correlation of electron and positron spin, providing complete description of polarization effects in strong-field

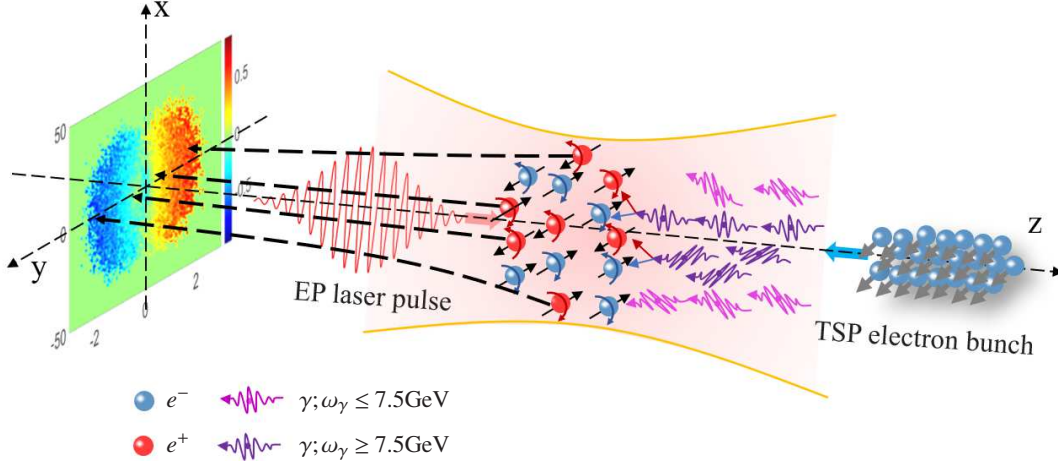


FIG. 3. Schemes of producing polarized positrons via nonlinear Compton scattering of an initially transversely polarized electrons off a strong elliptically polarized laser pulse. The energetic gamma-photons in  $\theta^y < 0$  region have high polarizations up to  $\xi_3 = 1$ , resulting in a reduction even reverse of polarization of positrons in small angle region.

QED processes. In each simulation step, one calculates the total emission rate to determine the occurrence of a photon emission, and the pair production rate to determine the pair production event, using the common QED Monte Carlo stochastic algorithm<sup>40–42</sup>. The spins of electron/positron after emission and creation are determined by the polarization-resolved emission probability of Sec. II.A and pair production probability of Sec. II.B, respectively, according to the stochastic algorithm. The electron/positron spin instantaneously collapses into one of its basis states defined with respect to the instantaneous spin quantization axis (SQA), which is chosen according to the properties of the scattering process. Moreover, since the probability of no emission is also polarization resolved and asymmetric along arbitrary SQA, it is necessary to include the spin variation between emissions induced by radiative polarization, besides spin precession governed by the Thomas-Bargmann-Michel-Telegdi equation<sup>57–59</sup>; for more details, see<sup>25</sup>. The polarization of the emitted photon is determined with a similar stochastic procedure, which also has been used in laser-plasma simulation codes<sup>60</sup>.

### III. SIMULATION RESULT

Recently, various schemes have been proposed to produce transversely polarized positrons via strong lasers, however, neglecting the polarization of photon. Here, we proceed to investigate the photon polarization effects on transverse polarization of positrons with the fully polarization resolved Monte-Carlo method, and compare the result with that obtained by the unpolarized photon model. A PW laser with intensity  $\xi_0 = \frac{|e|E_0}{m\omega} = 100$  ( $I = 10^{22} \text{W/cm}^2$ ) counterpropagates with a relativistic electron beam with an energy of  $\varepsilon_0 = 10 \text{ GeV}$ , the setup is shown in Fig. 3. The wavelength of the laser is  $\lambda_0 = 1 \mu\text{m}$ , the beam waist size  $w = 5\lambda_0$ , the pulse duration  $\tau_p = 8T$  and the ellipticity  $\epsilon = 0.03$ . The electron beam con-

sists of  $N_e = 6 \times 10^6$  electrons, with the beam length  $L_e = 5\lambda_0$ , the beam radius  $r_e = \lambda_0$ , the energy divergence  $\Delta\varepsilon = 0.06$ , the angular divergences  $\Delta\theta = 0.3 \text{ mrad}$  and  $\Delta\phi = 1 \text{ mrad}$ . The initial electron beam is fully polarized along  $y$ -direction.

The impact of the photon polarization on the pair production is elucidated in Fig. 4. The positron density decreases when photon polarization is resolved in both photon emission and pair production processes, as shown in Fig. 4(a),(c),(e). The difference in positron density of using polarization resolved or unresolved treatment is approximately  $(N(\xi) - N(0))/N(0) \approx 12.6\%$ . More importantly, the  $y$ -component of polarization  $\bar{\zeta}_y$  decreases dramatically at small angles, even showing reversal of polarization direction, see Fig. 4(d). As a consequence, the symmetric angular distribution of  $\bar{\zeta}_y$  near  $\theta_y = 0$  is distorted when the intermediate photon polarization is considered, as shown in Fig. 4(f). The angular distribution of  $\bar{\zeta}_y$  oscillates around small angle region, instead of a monotone increase as in the photon polarization averaged case. The average polarization of positron beam decreases by  $[\bar{\zeta}_y(\xi) - \bar{\zeta}_y(0)]/\bar{\zeta}_y(0) \approx 35\%$ .

To understand the effects of photon polarization on pair production, we investigate the polarization of emitted photons in  $\theta_y^y > 0$  and  $\theta_y^y < 0$  separately, as shown in Fig. 5. The photon density emitted within the angular region  $\theta_y^y < 0$  is larger than at  $\theta_y^y > 0$ , especially in high energy region, as shown in Fig. 5(a). When an electron with  $\vec{\zeta}_i = \vec{b}$  counterpropagate to the laser field, the direction of the instantaneous quantization axis is  $\vec{n} = \vec{\zeta}^f / |\vec{\zeta}^f|^{25}$  with

$$\vec{\zeta}^f = \frac{(2f_2 - f_1)\vec{\zeta}_i - \frac{\omega}{\varepsilon'}\vec{b}f_3 + \frac{\omega}{\varepsilon'\varepsilon}[f_2 - f_1](\vec{\zeta}_i\vec{v})\vec{v}}{\frac{\varepsilon^2 + \varepsilon'^2}{\varepsilon'\varepsilon}f_2 - f_1 - \frac{\omega}{\varepsilon}\vec{\zeta}_i\vec{b}f_3}, \quad (17)$$

which is mostly along  $B_y$ , and changes sign every half-cycle. For the electron with initial spin  $\zeta_y = 1$ , its spin is parallel (spin up) and anti-parallel (spin down) to the quantization axis in the half-cycles with  $B_y > 0$  and  $B_y < 0$ , respectively. The emission

probability is larger when electron is spin down before the emission, as shown in Fig. 5(a), which is in accordance with the analysis of the spin resolved probability given in Fig. 1(a). Further, the photon emission direction is parallel to the momentum of the emitting particle, and the photons emitted in  $B_y > 0$  ( $B_y < 0$ ) propagate with  $p_y < 0$  ( $p_y > 0$ ), respectively, because the oscillation phase of  $p_y$  has a  $\pi$ -delay with respect to  $B_y$ . Therefore, the electrons emit photons with  $\theta_y^\gamma > 0$  at  $B_y > 0$  and emit photons with  $\theta_y^\gamma < 0$  at  $B_y < 0$ . The latter has higher emitted photon number than former due to the larger emission probability  $W_{r\downarrow} > W_{r\uparrow}$ , as explained above. More importantly, the electrons with spin-up (spin-down) have a higher probability to emit photons with  $-1 < \xi_3 < 0.5$  ( $0.5 < \xi_3 < 1$ ). Therefore, the radiation with  $\theta_y > 0$  mainly comes from photon emission at  $B_y > 0$ , and has polarization  $-1 < \xi_3 < 0.5$ . While the radiation at  $\theta_y < 0$  comes from photon emission at  $B_y < 0$ , which has polarization  $0.5 < \xi_3 < 1$ , as shown in Fig. 5(b).

The fringes in the angular distribution, seen in Figs. 5(c)-(e), are due to the radiation in different laser cycles. As shown in Fig. 5(b),  $\bar{\xi}_3$  in high energy region is positive for spin down electrons while negative for spin up electrons. However, since the radiation is dominated by low energy photons with  $\xi_3 \sim 0.55$ , the angular distribution of the photon polarization in Fig. 5(d) is also dominated by  $\xi_3 \sim 0.55$ . Nevertheless, after filtering the low energy emissions, the correlation of photon polarization and emission angle can be seen in Figs. 5(e) and (f). As expected, the photons distributed in  $\theta_y^\gamma < 0$  have  $\bar{\xi}_3 < 0$ , while in the region  $\theta_y^\gamma > 0$  the polarization is  $\bar{\xi}_3 > 0$ . Since the pairs are produced mostly by energetic photons, the distinct polarization properties of high energy photons in  $\theta_y^\gamma < 0$  and  $\theta_y^\gamma > 0$  break the symmetric angular distribution of polarization.

The separation of positron polarization along propagation direction can be explained<sup>32</sup>, taking into account that the final momentum of the created electron (positron) is determined by the laser vector-potential  $A_y(t_p)$  at the creation moment  $t_p$ :  $p_f = p_i + eA_y(t_p)$ , where  $p_i$  is the momentum inherited from parent photon, with the vanishing average value  $\bar{p}_i = 0$ . On the other hand, when the photon is linearly polarized with  $(0, 0, \xi_3)$ , the SQA for pair production of such a photon is along the laser magnetic field direction,  $\vec{n} = \vec{\zeta}_+^{f,\xi} / |\vec{\zeta}_+^{f,\xi}| = \vec{b}$ . Therefore, the positrons produced at  $A_y(t_p) < 0$  obtain a final momentum  $p_f \approx eA_y(t_p) > 0$  and is polarized along  $\zeta_y > 0$ , as the instantaneous SQA is along  $y > 0$  at  $t_p$ . Similarly, one has  $\zeta_y < 0$  when  $p_f < 0$ .

To reveal the origin of the abnormal polarization features in a small angle region, we artificially turn on pair production of photons with  $\theta_y^\gamma > 0$  and  $\theta_y^\gamma < 0$  separately. As shown in Fig. 5(b), the photons with  $\theta_y^\gamma < 0$  have  $\xi_3 \sim 1$  at high energy end of spectrum. Those hard photons have a higher probability to produce energetic positrons anti-parallel with magnetic field, as discussed in Sec. I.B, resulting in a reverse of polarization direction in small angle region and a overall decrease of averaged polarization of positrons, as shown in Fig. 6(b). Moreover, since the parent photon with  $\theta_y^\gamma < 0$  have  $\bar{p}_i < 0$ , the positrons distribution is slightly shifted towards  $\theta_y^+ < 0$ . Meanwhile, the polarization of hard photons at

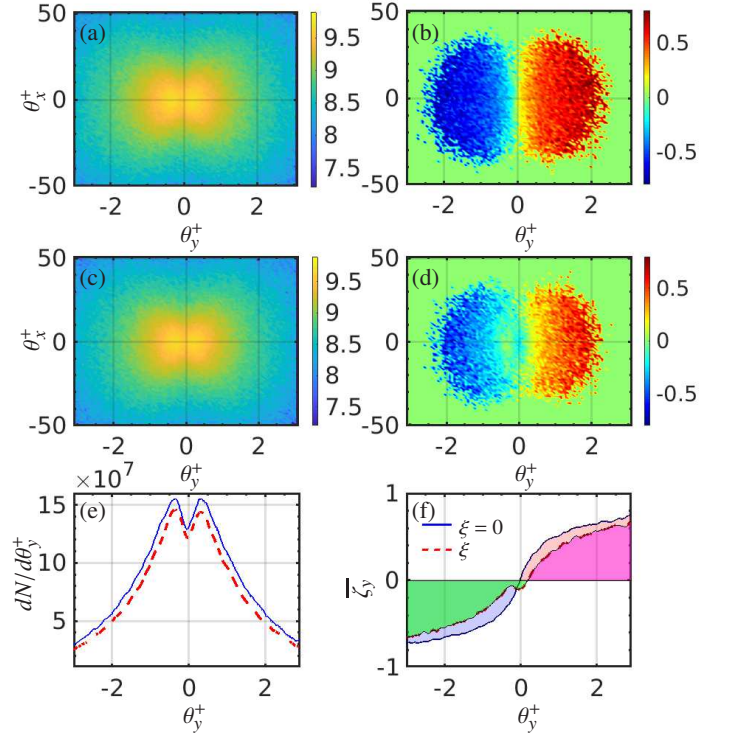


FIG. 4. Polarized positrons density distribution  $d^2N^+/d\theta_x^+d\theta_y^+$  ( $\text{rad}^{-2}$ ) (left column) and averaged polarization degree of  $y$  component  $\bar{\zeta}_y$  (right column) versus  $\theta_x^+ = p_x/p_z$  (rad) and  $\theta_y^+ = p_y/p_z$  (rad) for photon polarization unresolved (top row) and resolved (middle row) pair production. (bottom row) Polarized positrons density distribution  $dN/d\theta_y$  ( $\text{rad}^{-1}$ ) versus  $\theta_y$  (rad) for unresolved (solid line) and resolved photon polarization (dotted line); Averaged polarization degree  $\bar{\zeta}_y$  versus  $\theta_y$  (rad) for unresolved (dashed line) and resolved photon polarization (dash-dot line).

$\theta_y^\gamma > 0$  side is reaching to  $\xi_3 \sim -1$  [Fig. 5(b)]. If these photons are collected to produce pairs, highly polarized positrons could be achieved due to the highly domination of the spin-up positrons,  $dW_{\downarrow\uparrow}(\xi_3 = -1) \gg dW_{\downarrow\uparrow}(\xi_3 = 0)$ . In the present case, the  $\bar{\zeta}_y$  of positrons produced by photons with  $\theta_y^\gamma > 0$  increases monotonously with  $\theta_y^+$ , and the angular distribution shift slightly towards  $\theta_y^+ > 0$ . Since the pair production probability is inversely proportional to  $\xi_3$ , and the photons with  $\theta_y^\gamma < 0$  have larger  $\bar{\xi}_3$  than those with  $\theta_y^\gamma > 0$ , therefore, more positrons are produced at  $\theta_y^+ > 0$ , as shown in Fig. 6(a). Thus, the domination of pair production of photons in  $\theta_y^\gamma < 0$  and  $\bar{p}_i < 0$  result in a decrease of the polarization of the positron beam and an asymmetric angular distribution of polarization.

#### IV. CONCLUSION

We have investigated the photon polarization effects on pair production in nonlinear Breit-Wheeler process via a newly developed Monte Carlo method employing the fully polarization resolved quantum probabilities. We show that the

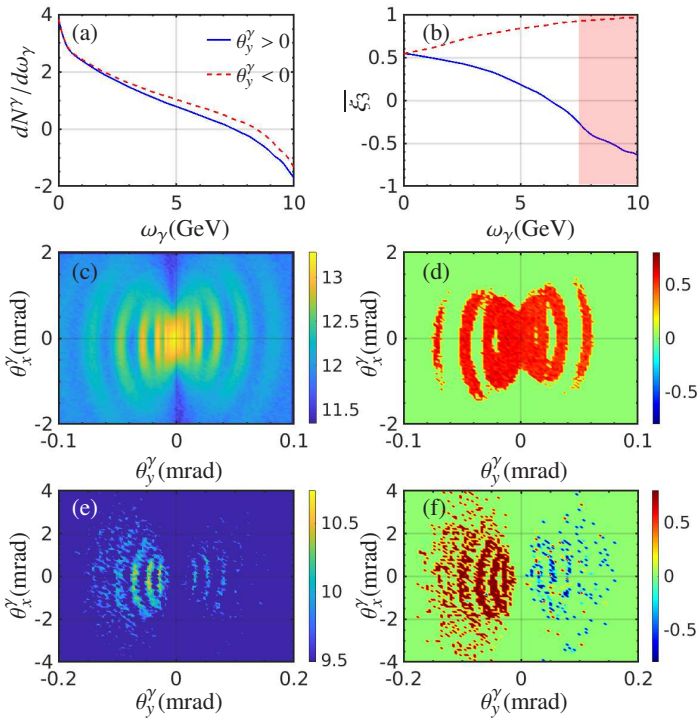


FIG. 5. (top row): (a)  $\log_{10}dN^\gamma/d\omega_\gamma$ , and (b) averaged Stokes parameter  $\bar{\xi}_3$  of gamma-photons emitted in  $\theta_y^\gamma > 0$  (solid line) and  $\theta_y^\gamma < 0$  (dashed line) vs photon energy  $\omega_\gamma$  in  $|\theta_x|, |\theta_y| < 10$  mrad. (middle row): (c) Angular distribution of  $d^2N^\gamma/d\theta_x^\gamma d\theta_y^\gamma$  ( $\text{rad}^{-2}$ ), and (d)  $\bar{\xi}_3$  vs  $\theta_x^\gamma = k_x/k_z$  and  $\theta_y^\gamma = k_y/k_z$ . (bottom row): (e) Angular distribution of  $d^2N^\gamma/d\theta_x^\gamma d\theta_y^\gamma$  ( $\text{rad}^{-2}$ ), and (f)  $\bar{\xi}_3$  for photons with energy  $\varepsilon > 7.5$  GeV [shaded red in (b)].

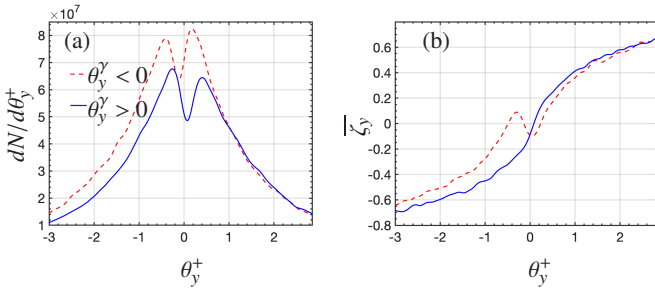


FIG. 6. (a) Polarized positron density distribution  $dN/d\theta_y^+$  ( $\text{rad}^{-1}$ ) vs positron polar angle  $\theta_y^+$  (rad) for positrons produced by photon with  $\theta_y^\gamma > 0$  (solid line) and  $\theta_y^\gamma < 0$  (dotted line); (b) Averaged polarization degree  $\bar{\zeta}_y$  versus  $\theta_y^+$  (rad) for positrons produced by photon with  $\theta_y^\gamma > 0$  (solid line) and  $\theta_y^\gamma < 0$  (dotted line).

longitudinal polarization of produced positrons is solely induced by the photon polarization. While the transverse polarization of positrons could either increase, decrease or even be unchanged determined by the polarization of intermediate gamma-photons. For the interaction of initially transversely polarized electrons and an elliptically polarized laser, both the polarization degree and density of positrons are reduced when the polarization of the intermediate photons are accounted for. This is because the photons emitted during nonlinear Compton

process are partially polarized along electric field direction with  $\bar{\xi}_3 \approx 0.55$ . The hard photons in  $\theta_y^\gamma < 0$  have even higher polarization  $\bar{\xi}_3 \sim 1$ , causing the energetic positrons produced in small angle region reverse the polarization direction. If one separates the intermediate hard gamma-photons within  $\theta_y^\gamma > 0$ , the polarization of positrons will be highly enhanced due to the domination of  $dW_{\uparrow}$  probabilities through the spectrum. Our results confirm that the important role of the intermediate photon polarization during strong-field QED process and should be accounted for in designing and optimizing a realistic laser driven polarized positron source. Moreover, the measurement of the correlated electron and positron polarization in pair production process can shed light on the intermediate interaction dynamics, in particular, on the polarization properties of intermediate photons.

<sup>1</sup>E. Voutier, “Physics potential of polarized positrons at the jefferson laboratory,” arXiv preprint arXiv:1412.1249 (2014).

<sup>2</sup>Q. Collaboration et al., “First determination of the weak charge of the proton,” Phys. Rev. Lett **111**, 141803 (2013).

<sup>3</sup>B. A. Mecking, G. Adams, S. Ahmad, E. Anciant, M. Anghinolfi, B. Asavapibhop, G. Asryan, G. Audit, T. Auger, H. Avakian, et al., “The cebaf large acceptance spectrometer (clas),” Nuclear Instruments and Methods in Physics Research Section A: Accelerators, Spectrometers, Detectors and Associated Equipment **503**, 513–553 (2003).

<sup>4</sup>A. Sokolov and M. Ternov, “On polarization and spin effects in the theory of synchrotron radiation,” in Sov. Phys.-Dokl., Vol. 8 (1964) pp. 1203–1205.

<sup>5</sup>I. Ternov, “Synchrotron radiation,” Physics-Uspekhi **38**, 409 (1995).

<sup>6</sup>V. Baier and V. Katkov, “Radiational polarization of electrons in inhomogeneous magnetic field,” Physics Letters A **24**, 327–329 (1967).

<sup>7</sup>Bař, “Radiative polarization of electrons in storage rings,” .

<sup>8</sup>Y. S. Derbenev and A. Kondratenko, “Polarization kinetics of particles in storage rings,” Sov. Phys. JETP **37** (1973).

<sup>9</sup>I. Sakai, T. Aoki, K. Dobashi, M. Fukuda, A. Higurashi, T. Hirose, T. Iimura, Y. Kurihara, T. Okugi, T. Omori, et al., “Production of high brightness  $\gamma$  rays through backscattering of laser photons on high-energy electrons,” Physical Review Special Topics-Accelerators and Beams **6**, 091001 (2003).

<sup>10</sup>T. Omori, M. Fukuda, T. Hirose, Y. Kurihara, R. Kuroda, M. Nomura, A. Ohashi, T. Okugi, K. Sakaue, T. Saito, et al., “Efficient propagation of polarization from laser photons to positrons through compton scattering and electron-positron pair creation,” Physical review letters **96**, 114801 (2006).

<sup>11</sup>X. Ji, “Deeply virtual compton scattering,” Physical Review D **55**, 7114 (1997).

<sup>12</sup>A. Potylitsin, “Production of polarized positrons through interaction of longitudinally polarized electrons with thin targets,” Nuclear Instruments and Methods in Physics Research Section A: Accelerators, Spectrometers, Detectors and Associated Equipment **398**, 395–398 (1997).

<sup>13</sup>Y.-F. Li, R. Shaisultanov, Y.-Y. Chen, F. Wan, K. Z. Hatsagortsyan, C. H. Keitel, and J.-X. Li, “Polarized ultrashort brilliant multi-gev  $\gamma$  rays via single-shot laser-electron interaction,” Physical review letters **124**, 014801 (2020).

<sup>14</sup>C. Danson, D. Hillier, N. Hopps, and D. Neely, “Petawatt class lasers worldwide,” High power laser science and engineering **3** (2015).

<sup>15</sup>V. Yanovsky, V. Chvykov, G. Kalinchenko, P. Rousseau, T. Planchon, T. Matsuoka, A. Maksimchuk, J. Nees, G. Cheriaux, G. Mourou, et al., “Ultra-high intensity-300-tw laser at 0.1 hz repetition rate,” Optics Express **16**, 2109–2114 (2008).

<sup>16</sup>J. W. Yoon, Y. G. Kim, I. W. Choi, J. H. Sung, H. W. Lee, S. K. Lee, and C. H. Nam, “Realization of laser intensity over 1023 w/cm<sup>2</sup>,” Optica **8**, 630–635 (2021).

<sup>17</sup>The Vulcan facility, <http://www.clf.stfc.ac.uk/Pages/TheVulcan-10-Petawatt-Project.aspx>.

<sup>18</sup>The Extreme Light Infrastructure (ELI), <http://www.elibeams.eu/en/facility/lasers/>.

<sup>19</sup>Exawatt Center for Extreme Light Studies (XCELS), <http://www.xcels.iapras.ru/>.

- <sup>20</sup>W. Leemans, A. Gonsalves, H.-S. Mao, K. Nakamura, C. Benedetti, C. Schroeder, C. Tóth, J. Daniels, D. Mittelberger, S. Bulanov, *et al.*, “Multi-gev electron beams from capillary-discharge-guided subpetawatt laser pulses in the self-trapping regime,” *Physical review letters* **113**, 245002 (2014).
- <sup>21</sup>A. Gonsalves, K. Nakamura, J. Daniels, C. Benedetti, C. Pieronek, T. De Raadt, S. Steinke, J. Bin, S. Bulanov, J. Van Tilborg, *et al.*, “Petawatt laser guiding and electron beam acceleration to 8 gev in a laser-heated capillary discharge waveguide,” *Physical review letters* **122**, 084801 (2019).
- <sup>22</sup>V. Ritus, “Quantum effects of the interaction of elementary particles with an intense electromagnetic field,” *Journal of Soviet Laser Research* **6**, 497–617 (1985).
- <sup>23</sup>F. Wan, R. Shaisultanov, Y.-F. Li, K. Z. Hatsagortsyan, C. H. Keitel, and J.-X. Li, “Ultrarelativistic polarized positron jets via collision of electron and ultraintense laser beams,” *Physics Letters B* **800**, 135120 (2020).
- <sup>24</sup>Y.-Y. Chen, P.-L. He, R. Shaisultanov, K. Z. Hatsagortsyan, and C. H. Keitel, “Polarized positron beams via intense two-color laser pulses,” *Physical review letters* **123**, 174801 (2019).
- <sup>25</sup>Y.-F. Li, Y.-Y. Chen, W.-M. Wang, and H.-S. Hu, “Production of highly polarized positron beams via helicity transfer from polarized electrons in a strong laser field,” *Physical Review Letters* **125**, 044802 (2020).
- <sup>26</sup>D. Seipt and B. King, “Spin- and polarization-dependent locally-constant-field-approximation rates for nonlinear compton and breit-wheeler processes,” *Phys. Rev. A* **102**, 052805 (2020).
- <sup>27</sup>A. Ilderton, B. King, and S. Tang, “Loop spin effects in intense background fields,” **102**, 076013 (2020).
- <sup>28</sup>V. Dinu and G. Torgrimsson, “Approximating higher-order nonlinear qed processes with first-order building blocks,” *Phys. Rev. D* **102**, 016018 (2020).
- <sup>29</sup>G. Torgrimsson, “Loops and polarization in strong-field QED,” *New J. Phys.* **23**, 065001 (2021).
- <sup>30</sup>D. Seipt, D. Del Sorbo, C. P. Ridgers, and A. G. Thomas, “Ultrafast polarization of an electron beam in an intense bichromatic laser field,” *Physical Review A* **100**, 061402 (2019).
- <sup>31</sup>H.-H. Song, W.-M. Wang, J.-X. Li, Y.-F. Li, and Y.-T. Li, “Spin-polarization effects of an ultrarelativistic electron beam in an ultraintense two-color laser pulse,” *Physical Review A* **100**, 033407 (2019).
- <sup>32</sup>Y.-F. Li, R. Shaisultanov, K. Z. Hatsagortsyan, F. Wan, C. H. Keitel, and J.-X. Li, “Ultrarelativistic electron-beam polarization in single-shot interaction with an ultraintense laser pulse,” *Physical review letters* **122**, 154801 (2019).
- <sup>33</sup>B. King, N. Elkina, and H. Ruhl, “Photon polarization in electron-seeded pair-creation cascades,” *Physical Review A* **87**, 042117 (2013).
- <sup>34</sup>F. Wan, Y. Wang, R.-T. Guo, Y.-Y. Chen, R. Shaisultanov, Z.-F. Xu, K. Z. Hatsagortsyan, C. H. Keitel, and J.-X. Li, “High-energy  $\gamma$ -photon polarization in nonlinear breit-wheeler pair production and  $\gamma$  polarimetry,” *Physical Review Research* **2**, 032049 (2020).
- <sup>35</sup>I. Gol’dman, “Intensity effects in compton scattering,” *Sov. Phys. JETP* **19**, 954 (1964).
- <sup>36</sup>A. Nikishov and V. Ritus, “Quantum processes in the field of a plane electromagnetic wave and in a constant field. i,” *Sov. Phys. JETP* **19**, 529–541 (1964).
- <sup>37</sup>G. L. Kotkin, V. G. Serbo, and V. I. Telnov, “Electron (positron) beam polarization by Compton scattering on circularly polarized laser photons,” *Phys. Rev. ST Accel. Beams* **6**, 11001 (2003).
- <sup>38</sup>D. Y. Ivanov, G. L. Kotkin, and V. G. Serbo, “Complete description of polarization effects in emission of a photon by an electron in the field of a strong laser wave,” *Eur. Phys. J. C* **36**, 127–145 (2004).
- <sup>39</sup>D. Y. Ivanov, G. L. Kotkin, and V. G. Serbo, “Complete description of polarization effects in,” *Eur. Phys. J. C* **40**, 27–40 (2005).
- <sup>40</sup>C. P. Ridgers, J. G. Kirk, R. Ducloux, T. Blackburn, C. Brady, K. Bennett, T. Arber, and A. Bell, “Modelling gamma-ray photon emission and pair production in high-intensity laser–matter interactions,” *Journal of computational physics* **260**, 273–285 (2014).
- <sup>41</sup>N. Elkina, A. Fedotov, I. Y. Kostyukov, M. Legkov, N. Narozhny, E. Nerush, and H. Ruhl, “Qed cascades induced by circularly polarized laser fields,” *Physical Review Special Topics-Accelerators and Beams* **14**, 054401 (2011).
- <sup>42</sup>D. Green and C. Harvey, “Simla: Simulating particle dynamics in intense laser and other electromagnetic fields via classical and quantum electrodynamics,” *Computer Physics Communications* **192**, 313–321 (2015).
- <sup>43</sup>V. Katkov, V. M. Strakhovenko, *et al.*, Electromagnetic processes at high energies in oriented single crystals (World Scientific, 1998).
- <sup>44</sup>V. Dinu, C. Harvey, A. Ilderton, M. Marklund, and G. Torgrimsson, “Quantum radiation reaction: from interference to incoherence,” *Physical review letters* **116**, 044801 (2016).
- <sup>45</sup>A. Di Piazza, M. Tamburini, S. Meuren, and C. Keitel, “Implementing nonlinear compton scattering beyond the local-constant-field approximation,” *Physical Review A* **98**, 012134 (2018).
- <sup>46</sup>A. Ilderton, B. King, and D. Seipt, “Extended locally constant field approximation for nonlinear compton scattering,” *Physical Review A* **99**, 042121 (2019).
- <sup>47</sup>T. Podszus and A. Di Piazza, “High-energy behavior of strong-field qed in an intense plane wave,” *Physical Review D* **99**, 076004 (2019).
- <sup>48</sup>A. Ilderton, “Note on the conjectured breakdown of qed perturbation theory in strong fields,” *Physical Review D* **99**, 085002 (2019).
- <sup>49</sup>A. Di Piazza, M. Tamburini, S. Meuren, and C. H. Keitel, “Improved local-constant-field approximation for strong-field qed codes,” *Physical Review A* **99**, 022125 (2019).
- <sup>50</sup>A. Gonoskov, S. Bastrakov, E. Efimenko, A. Ilderton, M. Marklund, I. Meyerov, A. Muraviev, A. Sergeev, I. Surmin, and E. Wallin, “Extended particle-in-cell schemes for physics in ultrastrong laser fields: Review and developments,” *Physical review E* **92**, 023305 (2015).
- <sup>51</sup>B. King and S. Tang, “Nonlinear compton scattering of polarized photons in plane-wave backgrounds,” *Physical Review A* **102**, 022809 (2020).
- <sup>52</sup>T. N. Wistisen and A. Di Piazza, “Numerical approach to the semiclassical method of radiation emission for arbitrary electron spin and photon polarization,” *Phys. Rev. D* **100**, 116001 (2019).
- <sup>53</sup>T. N. Wistisen, “Numerical approach to the semiclassical method of pair production for arbitrary spins and photon polarization,” *Physical Review D* **101**, 076017 (2020).
- <sup>54</sup>V. Baier and V. Katkov, “Quantum radiation theory in inhomogeneous external fields,” .
- <sup>55</sup>T. Blackburn, A. Ilderton, C. Murphy, and M. Marklund, “Scaling laws for positron production in laser–electron-beam collisions,” *Physical Review A* **96**, 022128 (2017).
- <sup>56</sup>O. Olugh, Z.-L. Li, B.-S. Xie, and R. Alkofer, “Pair production in differently polarized electric fields with frequency chirps,” *Physical Review D* **99**, 036003 (2019).
- <sup>57</sup>L. H. Thomas, “The motion of the spinning electron,” *Nature* **117**, 514–514 (1926).
- <sup>58</sup>L. H. Thomas, “I. the kinematics of an electron with an axis,” *The London, Edinburgh, and Dublin Philosophical Magazine and Journal of Science* **3**, 1–22 (1927).
- <sup>59</sup>V. Bargmann, L. Michel, and V. Telegdi, “Precession of the polarization of particles moving in a homogeneous electromagnetic field,” *Physical Review Letters* **2**, 435 (1959).
- <sup>60</sup>K. Xue, Z.-K. Dou, F. Wan, T.-P. Yu, W.-M. Wang, J.-R. Ren, Q. Zhao, Y.-T. Zhao, Z.-F. Xu, and J.-X. Li, “Generation of highly-polarized high-energy brilliant  $\gamma$ -rays via laser-plasma interaction,” *Matter and Radiation at Extremes* **5**, 054402 (2020).